Macromolecules **1992,** *25,* 2086–2092

Effects of Removing THF from the $TiCl_3(AA)/3MgCl_2/THF$ Catalyst System on the Ethylene–Propylene Copolymerization Mechanism

Ho-Sik Chang, Won-Deuk Song, Kyung-Jun Chu, and Son-Ki Ihm*

Department of Chemical Engineering, Korea Advanced Institute of Science and Technology, 373-1 Kusong-dong, Yusong-gu, Taejon, 305-701, Korea

Received September 6, 1991; Revised Manuscript Received December 11, 1991

ABSTRACT: $TiCl_3(AA)/MgCl_2/THF$ (T3ME) catalyst was prepared by reacting $TiCl_3(AA)$ and $MgCl_2$ in a solution of tetrahydrofuran (THF), and THF was removed from T3ME by diethylaluminum chloride to make four different catalysts with different THF contents (T3MED2, T3MED4, T3MED8, T3MED12). The investigation through XRD and ESR indicated that the removal of THF resulted in a change of the state of the Ti^{3+} species, isolated Ti^{3+} species for T3ME, T3MED2, and T3MED4 catalysts, and multinuclear Ti^{3+} species for T3MED12 and $TiCl_3(AA)$ catalysts. The ^{13}C NMR study showed that the microstructure of ethylene–propylene copolymers strongly depended upon the nature of Ti^{3+}. The activity and stereospecificity for homopolymerization depended on the THF content of the catalyst, and the molecular weight distribution of copolymer became broader with THF removal. Multinuclear Ti^{3+} species increased the relative reactivity of propylene in the copolymerization, and isolated Ti^{3+} species with vacancies favored the random insertion of propylene in the ethylene main chain.

Introduction

Highly active Ziegler-Natta catalyst systems, composed of titanium, magnesium, chlorine, and an electron donor, have been widely investigated for olefin polymerization.[1-5]

Especially for ethylene copolymerization with a 1-olefin comonomer such as propylene, 1-butene, and/or 1-hexene, the main interest has been focused on the relative activity of comonomers and the distribution of molecular weight and monomer composition of the copolymer.

Experiments have been oriented to analyze mostly the correlations between the stereospecificity and the relative activities of the monomers using the particular catalysts. Wu et al.[6] used $TiCl_4/MgCl_2$/ethyl benzoate (EB) catalyst produced by comilling, EB as external donor, and $AlEt_3$ as cocatalyst, and they showed that the isospecific sites produce the copolymer with lower ethylene content while the nonstereospecific sites give the copolymer with higher ethylene content. On the other hand, Soga et al.[7] used two different catalyst systems (aspecific catalyst composed of $TiCl_3/MgCl_2$ and $AlEt_3$ as cocatalyst, isospecific Solvay-type catalyst composed of $TiCl_3$ and $Cp_2Ti(CH_3)_2$ as cocatalyst), and they reported that the stereospecificity of catalyst affects neither the monomer reactivity ratio in the case of ethylene–propylene copolymerization nor the monomer distribution of the copolymer.

In the present study, the $TiCl_3(AA)/3MgCl_2/THF$ (T3ME) catalyst system was prepared through chemical reaction between $TiCl_3(AA)$ and $3MgCl_2$ in the THF solution[8] and used for ethylene–propylene copolymerization. Four catalysts (T3MED*X*, *X* = 2, 4, 8, 12) of the $TiCl_3(AA)/3MgCl_2/THF$ system having different THF contents were prepared by removing THF from the T3ME catalyst with diethylaluminum chloride (DEAC). With the present catalyst system it is expected that the complexity arising from the formation of surface complex (produced by comilling and chemical anchoring) and the additional difficulty arising from the different catalyst system could be minimized.

These catalysts were characterized by inductively coupled plasma spectrophotometer (ICP), gas chromatography (GC), X-ray diffractometer (XRD), and electron spin resonance spectrometer (ESR). The homo- and copolymerizations of ethylene and propylene at 40 °C in the presence of $AlEt_3$ under various propylene/ethylene mole ratios were carried out in a slurry phase over these catalysts. Copolymer was characterized by GPC, FT-IR, and ^{13}C NMR.

In this paper, the change of the initial state of Ti^{3+} species with THF removal from the T3ME was observed. The stereoregularity and activity of catalysts, the molecular weight distribution, and the composition and the microstructure of ethylene–propylene copolymers were discussed in terms of the status of the Ti^{3+} species in the $TiCl_3(AA)/3MgCl_2/THF$ catalyst system.

Experimental Section

Materials. Ethylene, propylene, and nitrogen were purified by removing traces of residual moisture and oxygen with columns packed with molecular sieve 5A (Aldrich) and oxygen scavenger (Fischer Ridox), respectively (Figure 1). Hexane (J. T. Baker) used in the polymerization reaction and in the catalyst preparation was dried by refluxing through a distillation column (1.5 m) over sodium metal under dry nitrogen. $TiCl_31/3AlCl_3$ ($TiCl_3(AA)$) (Toho titanium), anhydrous $MgCl_2$ (Toho titanium), anhydrous tetrahydrofuran (Aldrich), diethylaluminum chloride (DEAC) (1 M in hexane, Aldrich) and triethylaluminum ($AlEt_3$) (1 M in hexane, Aldrich) were used as received.

The designations T3, M, and E in the nomenclature for the catalysts and the complexes refer to $TiCl_3(AA)$, $MgCl_2$, and electron donor (THF), respectively. D refers to DEAC used to remove THF from the $TiCl_3(AA)/3MgCl_2/THF$ (T3ME) catalyst, and the number following D implies the amount of DEAC used (for more details, refer to the Catalyst Preparation).

Catalyst Preparation. (a) ME and T3E Complexes. $MgCl_2$ (25 mmol) was added to a 250-mL four-neck round-bottom flask fitted with a water condenser and magnetic stirrer. Anhydrous THF (125 mL) was added under nitrogen flow, and the $MgCl_2$/THF slurry was stirred rapidly under reflux until the slurry became a clean solution. This solution was transferred to a 1-L two-neck round-bottom flask fitted with a magnetic stirrer through a double-ended needle under nitrogen. Dry hexane (700 mL) was added to the transferred solution with vigorous stirring. Then, $MgCl_2$/THF (ME) complex slurry was separated from solution by decantation. The precipitate of ME complex was washed again with 700 mL of dry hexane, and the solvent was

---

* Author to whom correspondence should be addressed.

0024-9297/92/2225-2086\$03.00/0

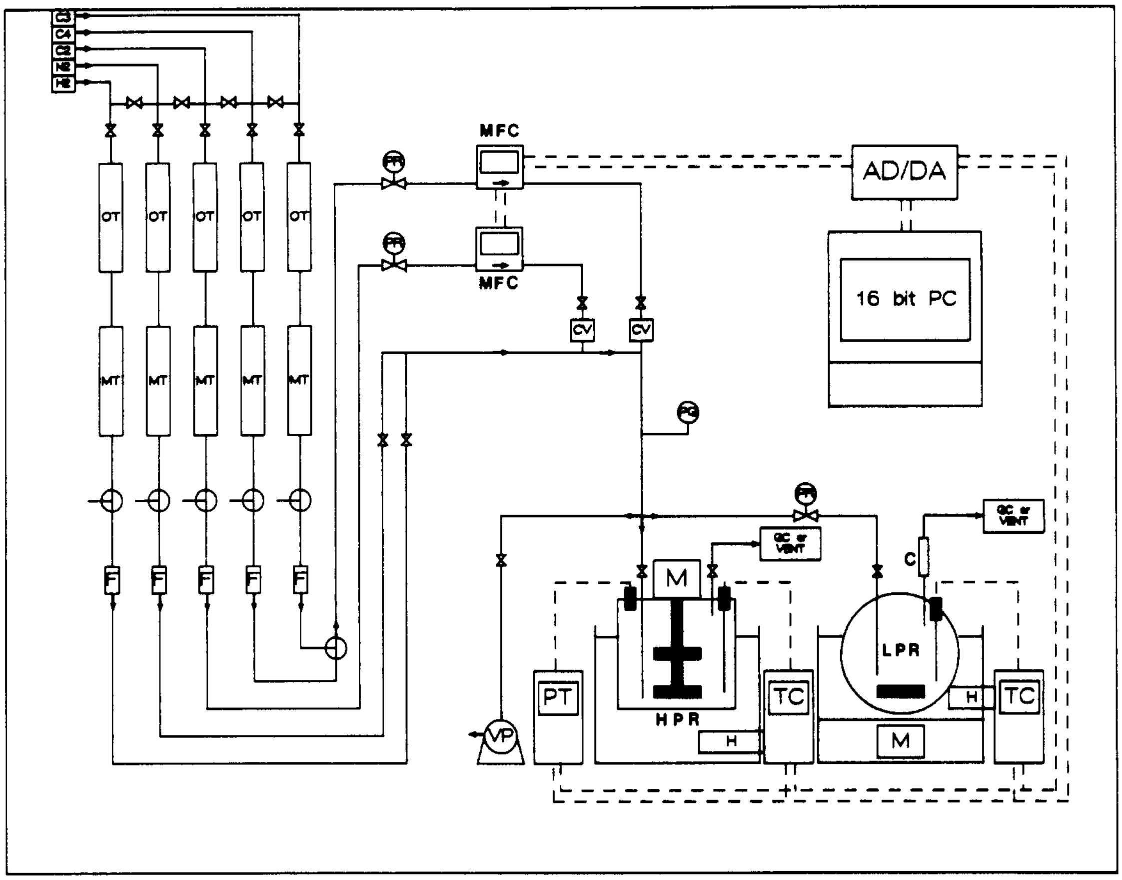

Figure 1. Apparatus for polymerization of semibatch and continuously purged copolymerization. AD/DA, analog–digital converter; C, condenser; CV, check value; F, filter; GC, gas chromatography; H, heater; HPL, high-pressure reactor; LPR, low-pressure reactor; M, motor; MFC, mass flow controller; MT, moisture trap; OT, oxygen trap; PG, pressure gauge; PR, pressure regulator; PT, pressure transducer; TC, temperature controller; VP, vacuum pump.

removed by decantation. The ME complex slurry was heated to 70 °C and dried with nitrogen for 4 h. The ME complex of a white free-flowing powder was stored in a drybox until used.

$TiCl_3(AA)/THF$ (T3E) complex was prepared in a similar manner except that $TiCl_3(AA)$ was used instead of $MgCl_2$. Blue free-flowing powder of T3E complex was stored in a drybox until used.

(b) T3ME Catalyst. $TiCl_3(AA)$ (8.35 mmol) was added to a 250-mL flask (reactor A), and 25 mmol of $MgCl_2$ was added to another 250-mL flask (reactor B). The system of reactor was the same as that used in the preparation of the ME complex. Amounts of 50 and 100 mL of anhydrous THF were added to reactors A and B, respectively. The two reactors were stirred until a clean solution was obtained, and then $TiCl_3(AA)/THF$ solution in reactor A was transferred dropwise over 10 min into reactor B. After reflux for 1 h, the $TiCl_3(AA)/3MgCl_2/THF$ solution in reactor B was transferred to a 1-L two-neck round-bottom flask under a slow nitrogen flow. The catalyst slurry was separated from solution, washed, and dried in a manner similar to the preparation of ME complex. $TiCl_3(AA)/3MgCl_2/THF$ (T3ME) catalyst in light blue free-flowing powder was stored in a drybox until used.

(c) T3MED*X* (*X* = 2, 4, 8, 12) Catalysts. About 3 g of T3ME catalyst and 150 mL of anhydrous hexane were added into a 250-mL reactor under nitrogen. Diethylaluminum chloride (DEAC) was added dropwise over 15 min at 25 °C. The amount of DEAC added was 0.2 mol/mol of THF contained in T3ME. The stirring was continued for 1 h, and then the catalyst slurry was decantated, washed with excess hexane, and dried under nitrogen at 70 °C over 4 h. T3MED2 catalyst of pale brown free-flowing powder was stored in a drybox under nitrogen until used.

T3MED4, T3MED8, and T3MED12 catalysts were prepared in a similar manner except for using 0.4, 0.8, and 1.2 mol of DEAC/mol of THF contained in the T3ME catalyst, respectively.

Table I
Elemental Composition (Weight Percent) of $MgCl_2/THF$ (ME), $TiCl_3(AA)/THF$ (T3E), $TiCl_3(AA)/3MgCl_2/THF$ (T3ME and T3MED*X*, *X* = 2, 4, 8, 12) Catalyst Systems and $TiCl_3(AA)$ (T3(AA)) Catalyst

catalyst	Ti[a]	Mg[a]	Al[a]	THF[a]
ME		11.3 (1)		54.7 (1.6)
T3E	10.5 (1)		1.9 (0.3)	55.0 (3.5)
T3ME	4.9 (1)	7.3 (2.9)	0.9 (0.3)	53.5 (7.2)
T3MED2	5.7 (1)	9.3 (3.2)	1.6 (0.2)	43.2 (5.0)
T3MED4	6.0 (1)	9.5 (3.1)	1.0 (0.3)	38.4 (4.3)
T3MED8	6.1 (1)	9.8 (3.2)	1.7 (0.5)	25.4 (2.8)
T3MED12	6.9 (1)	10.3 (3.0)	5.6 (1.5)	14.0 (1.4)

[a] Mole ratio to titanium or magnesium is shown in parentheses.

Catalyst Characterization. (a) Elemental Analysis of Catalysts. The amount of Ti, Mg, and Al metals in the catalysts was measured with ICP (ARL-3510). The content of THF in ME, T3E complexes and T3ME and T3MED*X* (*X* = 2, 4, 8, 12) catalysts after THF was extracted with acetone was measured by gas chromatograph (Varian 1420). The composition of each catalyst is given in Table I, where it can be seen that the content of THF decreases with the treatment by DEAC.

(b) Electron Spin Resonance (ESR). Catalyst sample was placed in a sample tube as dry solids under nitrogen. The ESR spectrum (Bruker ESP-300S spectrometer) was taken at 25 °C. The *g* values of ESR spectra were determined by referring to those of diphenylpicrylhydrazyl. Relative intensity (I) of the Ti^{3+} species on the ESR spectra was measured by approximately integrated spectra of catalysts as[9]

$$I \cong Y'_{\max}(\Delta H_{pp})^2$$

where $2Y'_{\max}$ is the peak-to-peak derivative amplitude and ΔH_{pp} is the peak-to-peak width.

(c) X-ray Diffractometry (XRD). Powder XRD (Rigaku CN-2155D2) was obtained at 30 keV and 25 °C. Powdered samples were loaded into a sample holder equipped with a special window under nitrogen, of which material was poly(ethylene terephthalate) or paraffin film.[10,11] Diffraction patterns of samples were taken in the range 8° < 2θ < 60°.

Polymerization. The schematic flow diagram of the polymerization unit is shown in Figure 1.

Homopolymerization was carried out in a high-pressure stainless steel reactor (HPR, 1 L) of semibatch type. For high-pressure polymerization, a specially designed glass vial including the prescribed amount of catalyst was introduced into the reaction vessel. After evacuation, 600 mL of anhydrous *n*-hexane and 30 mol of $AlEt_3$/mol of Ti in catalyst were added into the vessel under nitrogen purge. Propylene or ethylene was then charged into the reactor up to the reaction pressure at 40 °C. When the stirring was started, the glass vial was broken by the stirrer and the polymerization started. During the polymerization at 40 °C, the pressure was kept constant, and the reactor was agitated at 1000 rpm. The polymerization rate was estimated from the monomer consumption rate, which was measured by mass flow meter (MFC, Type 825 of Datametrics) connected to a 16-bit PC via an AD/DA converter (ADL 1100 of Analog Design).

Ethylene–propylene copolymerization was carried out under atmospheric condition in a glass reactor (LPR, 500 mL) by a continuously purged copolymerization (CPC) method.[12,13] For CPC, 200 mL of hexane was saturated at 40 °C with the gas mixture of ethylene and propylene, whose composition could be adjusted by the mass flow controller (MFC). The concentrations of ethylene and propylene in hexane were predicted by the Peng–Robinson equation.[14] Total flow rate of gas mixture was 2 L/min under 1 atm. After saturation, the copolymerization was initiated by introducing about 0.05 g of catalyst and $AlEt_3$ as cocatalyst with Al/Ti = 30. The reaction was stopped with ethanol after 15–20 min, and the copolymers were separated.

Polymer Characterization. The polymer products were melt-pressed into films, which were investigated with FT-IR (Bomem MB-102). The isotactic index of polypropylene was determined from the absorbance ratio of the peaks at 995 and 970 cm^{-1} by following the method proposed by Burfield and Loi.[15] The compositions of ethylene–propylene copolymers were estimated from the absorbance ratio of the peaks at 1376 and 1457 cm^{-1},[16] which were calibrated with the sequence distribution of monomers measured by ^{13}C NMR (Bruker AM 300 FT-NMR). The monomer composition in the copolymer obtained from FT-IR was used to estimate the reactivity ratio of each monomer.

^{13}C NMR spectra of copolymer were recorded at 120 °C and 75.469 MHz. The solution of ethylene–propylene copolymer was prepared in *o*-dichlorobenzene containing 25 vol % deuterated benzene (C_6D_6) as a locking material. Tetramethylsilane was used as an internal standard. The microstructure of copolymer was analyzed with ^{13}C NMR according to each of the methods reported by Randall[17] and Kakugo.[18]

The molecular weight distribution was measured by gel permeation chromatography (Waters 150CV) at 135 °C with 1,3,5-trichlorobenzene as solvent.

Results and Discussion

Structural Change Observed by XRD. It can be seen in Figure 2A that the XRD peak patterns of ME and T3E are different from those of their precursors (anhydrous $MgCl_2$ and $TiCl_3$(AA), respectively). This indicates that the anhydrous $MgCl_2$ and $TiCl_3$(AA) experience significant structural change through the interactions with THF. Keszler[10] reported that new bands of XRD were observed through addition of ethyl benzoate to $MgCl_2$.

$TiCl_3$(AA)/3$MgCl_2$/THF (T3ME) catalyst, which is the model catalyst for this study, shows a mixed XRD pattern of ME and T3E and seems to retain the characteristic peaks of ME especially at 2θ = 9.75, 20.38, and 32.38°.

Figure 2B shows the XRD patterns of T3ME, T3MED2, T3MED4, T3MED8, and T3MED12, the same sequence of which might provide information on the structural change through interaction with DEAC (and accordingly with the removal of THF). The characteristics of $MgCl_2$/THF (ME) structure have been retained in T3MED2 and T3MED4 but lost in T3MED8 and T3MED12. This might indicate that a small amount of DEAC (0.2 and 0.4 mol/mole of THF in T3ME) does not destroy the ME structure but that large amounts of DEAC (0.8 and 1.2 mol/mol of THF in T3ME) can destroy the ME structure.

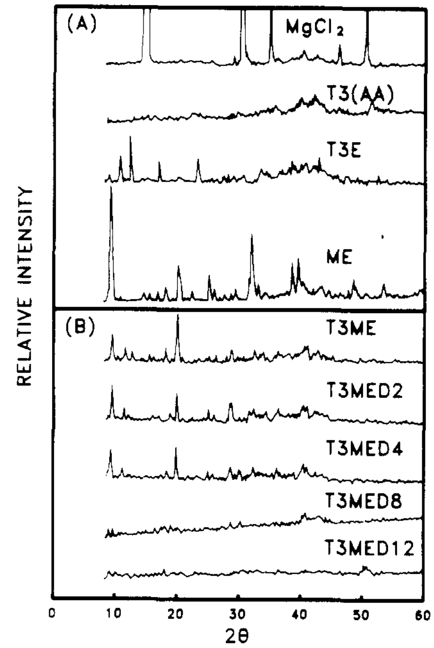

Figure 2. X-ray diffraction patterns of (A) $MgCl_2$, $TiCl_3$(AA)-(T3(AA)), $TiCl_3$(AA)/THF (T3E), and $MgCl_2$/THF (ME) and (B) $TiCl_3$(AA)/3$MgCl_2$/THF (T3ME and T3MED*X*, *X* = 2, 4, 8, 12) catalyst system.

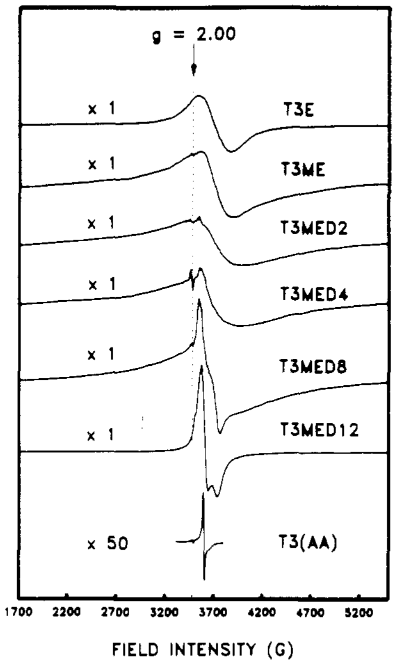

Figure 3. ESR spectra of $TiCl_3$(AA)/THF (T3E), $TiCl_3$(AA)/3$MgCl_2$/THF (T3ME and T3MED*X*, *X* = 2, 4, 8, 12) catalyst system and $TiCl_3$(AA)(T3(AA)) catalyst.

State of Ti^{3+} Species in $TiCl_3$(AA)/3$MgCl_2$/THF Catalyst System. Figure 3 and Table II show the characteristic ESR spectra of $TiCl_3$(AA), T3E, T3ME, and T3MED*X* (*X* = 2, 4, 8, 12) catalysts.

T3(AA) shows a very weak and anisotropic ESR spectrum. Zakharov[19] explained that less than 1 mol % of total titanium in $TiCl_3$(AA) can be detected by ESR,

Table II
ESR Data on Ti^{3+} Species in the $TiCl_3(AA)/THF$ (T3E), $TiCl_3(AA)/3MgCl_2/THF$ (T3ME, T3MED*X* (*X* = 2, 4, 8, 12)) Catalyst Systems and $TiCl_3(AA)$ (T3(AA)) Catalyst

catalyst	*g* value	ΔH_{pp}(G)[b]	intensity[c]
T3E	$g = 1.880$	307.8	4.5×10^7
T3ME	$g = 1.880$	339.0	6.4×10^7
T3MED2	$g = 1.880$, F center[a]	435.5	7.9×10^7
T3MED4	$g = 1.882$, F center	393.5	7.6×10^7
T3MED8	$g_\perp = 1.961$ $g_\parallel = 1.854$	211.8	5.1×10^7
T3MED12	$g_\perp = 1.950$ $g_\parallel = 1.865$	165.1	3.0×10^7
T3(AA)	$g = 1.938$	17.4	4.5×10^3

[a] F center, $g \simeq 2.00$ (to indicate formation of vacancies). [b] ΔH_{pp}(G), peak-to-peak width. [c] Intensity of ESR signal (unit is arbitrary).

and Chien and Wu[20] reported that "ESR-silent" Ti^{3+} species are those bound to one or more other Ti^{3+} species.

T3E, however, has a very intense and isotropic ESR spectrum. This seems to be due to free isolated Ti^{3+} species in the T3E complex which was formed by dissolving the aggregate of $TiCl_3(AA)$ in THF.

T3ME, T3MED2, and T3MED4 also show very intense and isotropic spectra. The shapes of the spectra are similar to that of T3E, but F-center signals[21] are observed at the *g* value of 2.00. The free isolated Ti^{3+} species seem to be highly dispersed over the $MgCl_2/THF$ (ME) matrix, and the F-center signal indicates that the THF ligand occupying the vacant site of isolated Ti^{3+} species is removed by DEAC without the ME matrix being destroyed.

The shape of the ESR spectra for T3MED8 and T3MED12 is quite different from that for T3ME, T3MED2, and T3MED4. The axial symmetric spectra of T3MED8 and T3MED12 indicate that the Ti^{3+} species are firmly fixed in the matrix of $MgCl_2$.[20] Especially the F-center signal is very weak for T3MED8 and not found for T3MED12. It seems that the destruction of ME matrix due to excessive removal of THF allows the chlorine of $MgCl_2$ clusters to occupy the vacancies of Ti^{3+} species. Further destruction may result in the occupation of the vacancies of Ti^{3+} species by other $TiCl_3$ species.

It is believed that with THF removed by DEAC (from T3ME to T3MED12) the state of Ti^{3+} species changes from isolated Ti^{3+} to multinuclear Ti^{3+} species ($TiCl_3$ aggregates).

Stereospecificity of Catalysts. Figure 4 shows the activity of the $TiCl_3(AA)/3MgCl_2/THF$ catalyst system for propylene polymerization and the isotactic index (I.I.) of polypropylene obtained with the catalysts.

The stereospecificity (I.I.) of T3MED2 and T3MED4 is lower than that of T3ME, while that of T3MED12 is higher than that of T3MED4 and T3MED8. It is noted that the stereospecificity of $TiCl_3(AA)$ is much higher (I.I. = 75%). With THF removal from T3ME, the isolated Ti^{3+} species with vacancies tends to be nonstereospecific as in T3MED2 and T3MED4 catalysts and the multinuclear Ti^{3+} species become isospecific as in T3MED12 and $TiCl_3(AA)$ catalysts.

Activity for Homo- and Copolymerization of Ethylene and Propylene. The activity of $TiCl_3(AA)/3MgCl_2/THF$ catalysts is affected by removal of THF from T3ME catalyst as summarized in Table III.

The rate of ethylene homopolymerization increases with THF removal and then decreases. T3MED4 shows the highest rate among them. It can be seen that the rate of propylene polymerization increases with THF removal.

It is believed that the free isolated Ti^{3+} species as in T3ME, T3MED2, and T3MED4 favors ethylene polymerization while the multinuclear Ti^{3+} species as in T3MED12 and $TiCl_3(AA)$ favors propylene polymerization.

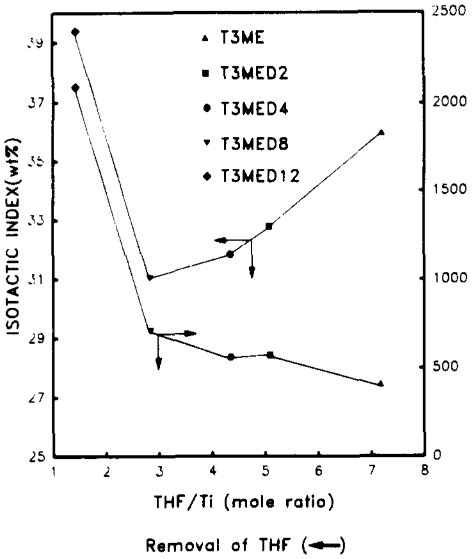

Figure 4. Effect of removing THF from T3ME on the activity of $TiCl_3(AA)/3MgCl_2/THF$ (T3ME and T3MED*X*, *X* = 2, 4, 8, 12) catalyst system and the isotactic index of polypropylene prepared with these catalysts (40 °C, Al/Ti = 30).

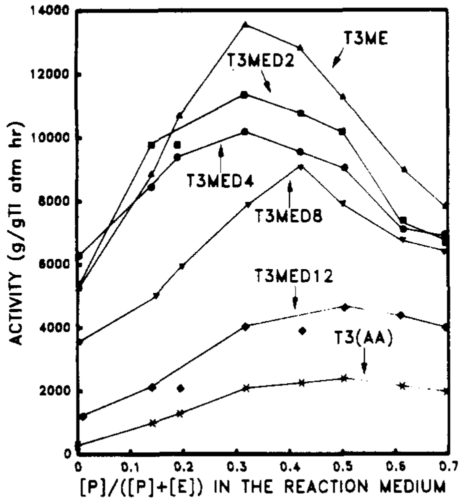

Figure 5. Activity as a function of monomer composition in the copolymerization over $TiCl_3(AA)/3MgCl_2/THF$ (T3ME and T3MED*X*, *X* = 2, 4, 8, 12) catalyst system and $TiCl_3(AA)$(T3-(AA)) catalyst (40 °C, Al/Ti = 30).

Table III
Activity of $TiCl_3/3MgCl_2/THF$ (T3ME, T3MED*X* (*X* = 2, 4, 8, 12)) Catalyst System in the Homopolymerization of Ethylene and Propylene (40 °C, Al/Ti = 30)

		activity, g of polymer/(g of Ti h atm)[a]	
catalyst	THF/Ti	ethylene	propylene
T3ME	7.2	5175	392
T3MED2	5.0	5231	571
T3MED4	4.3	6212	552
T3MED8	2.8	3525	706
T3MED12	1.4	1155	2079

[a] The activities for ethylene and propylene homopolymerization are obtained from Figures 4 and 5 ([P]/([P] + [E]) = 0), respectively.

Figure 5 shows the activity of ethylene–propylene copolymerization with varying monomer composition at 40 °C. The activity for copolymerization mostly decreases with THF removal. It is noted that each catalyst shows a maximum activity at a specific monomer composition,

Table IV
Normalized Area (Percent Area) of Each Peak on the ^{13}C NMR Spectra of Ethylene–Propylene Copolymers Prepared with $TiCl_3/3MgCl_2$/THF (T3ME, T3MED*X* (*X* = 2, 4, 8, 12)) Catalyst System and $TiCl_3$(AA) (T3(AA)) Catalyst (40 °C, Al/Ti = 30, [P]/([P] + [E]) = 0.5)

carbon type[a]	region,[b] ppm	catalyst T3ME	 T3MED2	 T3MED4	 T3MED8	 T3MED12	 T3(AA)	 T3(AA)[c]
$S\alpha\alpha$	Ta(45–48)	0.801	0.837	0.574	0.638	1.059	2.142	1.008
$S\alpha\gamma$ $S\alpha\delta$	Tb(36–39)	7.628	9.438	8.556	8.374	9.857	10.171	6.782
$T\delta\delta$	Tc(33.3)	3.420	4.122	3.563	3.393	3.808	3.877	3.119
$T\beta\delta$ $S\gamma\gamma$ $S\gamma\alpha$ $S\beta\beta$	Td(29.1–31.6)	77.326	72.628	75.518	75.762	69.860	67.272	77.955
$T\beta\beta$	Te(28–29.5)	0.000	0.000	0.000	0.000	1.351	1.324	0.867
$S\beta\delta$	Tf(27–28)	5.943	7.170	6.536	6.583	7.247	7.072	5.275
$S\beta\beta$	Tg(24–25)	0.655	0.805	0.665	0.659	0.921	1.253	0.596
$P\beta\beta$ $P\beta\delta$ $P\beta\gamma$	Th(19–22)	4.227	5.000	4.587	4.589	5.896	6.888	4.398
$P\beta\beta$[d]		0.000	0.000	0.000	0.000	0.459	0.263	0.079

[a] S, T, and P refer to secondary (methylene), tertiary (methine), and primary (methyl) carbons, respectively. The two Greek letter refer to the distance a given carbon is from neighboring methine carbon bearing methyl group. [b] The region will be used for the estimation of observed dyad–triad sequence distribution by the Randall method. [c] All of the copolymer samples except this T3(AA) were prepared at $M_P/M_E = 1$. This T3(AA) sample was prepared at $M_P/M_E = 4/6$. [d] The normalized area of $P\beta\beta$ in Th region.

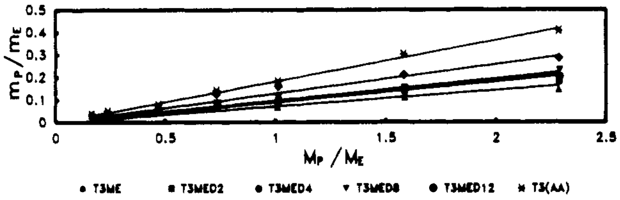

Figure 6. (m_P/m_E) vs (M_P/M_E) for ethylene–propylene copolymerization with $TiCl_3(AA)/3MgCl_2$/THF (T3ME and T3MED*X*, *X* = 2, 4, 8, 12) catalyst system and $TiCl_3$(AA) (T3(AA)) catalyst (40 °C, Al/Ti = 30).

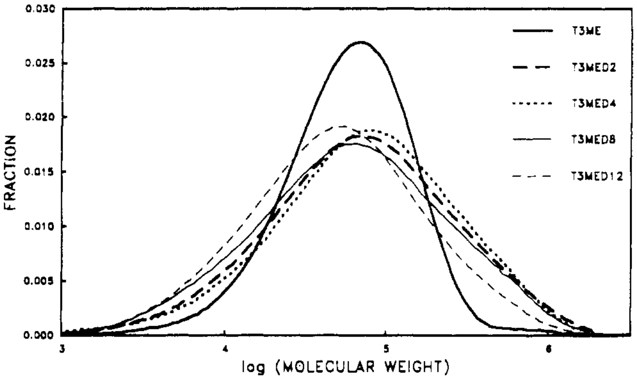

Figure 7. Molecular weight distribution of ethylene–propylene copolymers prepared with $TiCl_3/3MgCl_2$/THF (T3ME, T3MED*X*, *X* = 2, 4, 8, 12) catalyst system (40 °C, Al/Ti = 30, [P]/([P] + [E]) = 0.5).

i.e., T3ME at [P]/([P] + [E]) ≅ 0.3 and T3MED12 at [P]/([P] + [E]) ≅ 0.5.

It is often observed in ethylene copolymerization using the Ziegler–Natta catalyst that the addition of a small quantity of propylene markedly increases the polymerization activity. The propylene addition may result in the increase of propagation rate constant[22] and/or the number of active sites.[23]

Relative Reactivity of Propylene in the Copolymerization. The relative reactivity of monomers in the copolymerization is represented by the reactivity ratio of each monomer. The reactivity ratio can be estimated by two different approaches: the kinetic approach[24] and the statistical approach using the dyad and triad distribution obtained by ^{13}C NMR.[25] The kinetic approach requires data on the mole ratio of the two monomers in each copolymer and the reaction feed.

When the reactivity of ethylene is much higher than that of propylene, the reactivity ratio can be estimated by a modified Mayo–Lewis equation[26]

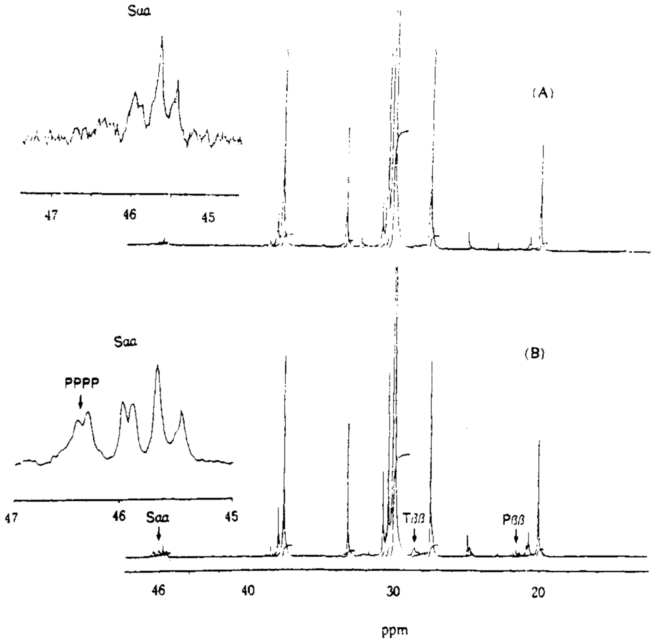

Figure 8. Typical ^{13}C NMR spectra of ethylene–propylene copolymers prepared with (A) T3ME and (B) T3MED12 (40 °C, Al/Ti = 30, [P]/([P] + [E]) = 0.5).

$$m_P/m_E = (1/r_E)(M_P/M_E)$$

where (m_P/m_E) and (M_P/M_E) are the mole ratios in the copolymer and reaction medium (hexane), respectively, and $r_E = k_{EE}/k_{EP}$ is the reactivity ratio constant (subscripts E and P stand for ethylene and propylene, respectively). This equation is valid for the ethylene-rich copolymers with a low propylene content.

Figure 6 shows the plottings of m_P/m_E against M_P/M_E for our catalysts. The slope $1/r_E$, is a measure of propylene reactivity for copolymerization. It can be found that the reactivity of propylene increases with THF removal in the following order:

$$\text{T3ME} < \text{T3MED2} < \text{T3MED4} \cong \text{T3MED8} < \text{T3MED12} < TiCl_3(\text{AA})$$

The reactivity of comonomer (propylene) seems to be favored by the multinuclear Ti^{3+} species rather than the isolated Ti^{3+} species and also by the isolated Ti^{3+} species with vacancies rather than the isolated Ti^{3+} species having vacancies occupied by the THF ligand, which is in turn

Table V

Observed Dyad–Triad Sequence Distribution (Mole Percent) of Ethylene–Propylene Copolymers Prepared with $TiCl_3$/$3MgCl_2$/THF (T3ME, T3MED*X* (X = 2, 4, 8, 12)) Catalyst System and $TiCl_3$(AA) (T3(AA)) Catalyst

catalyst	method	P	EE	EP	PP	EEE	PEE	PEP	EPE	PPE	PPP
T3ME	R[b]	9.3	83.1	15.2	1.7	76.9	12.4	1.4	7.2	0.8	1.3
	K[c]	10.0	81.8	16.5	1.7	74.8	12.6	1.7	7.3	3.6	0.0
T3MED2	R	11.2	79.4	18.8	1.8	71.7	15.4	1.7	8.7	1.4	1.1
	K	11.7	78.4	20.0	1.8	69.5	14.9	2.0	8.6	5.1	0.0
T3MED4	R	9.9	81.4	17.4	1.2	74.1	14.6	1.4	7.5	2.4	0.0
	K	10.2	80.7	18.0	1.2	73.3	13.8	1.7	7.5	3.8	0.0
T3MED8	R	9.9	81.6	17.1	1.2	74.4	14.3	1.4	7.1	2.8	0.0
	K	10.1	81.1	17.5	1.3	74.4	13.9	1.6	7.1	3.0	0.0
T3MED12	R	12.6	77.0	20.8	2.3	68.5	16.9	2.0	8.1	4.6	0.0
	K	12.4	77.4	20.3	2.3	67.0	14.8	2.2	7.9	5.3	2.8
T3(AA)	R	15.2	74.2	21.2	4.6	66.3	15.8	2.7	8.4	4.5	2.4
	K	15.7	73.3	22.1	4.7	64.2	14.8	3.1	8.2	6.8	2.8
T3(AA)[a]	R	9.2	83.7	14.2	2.1	77.9	11.7	1.2	6.5	1.1	1.5
	K	9.6	83.4	14.5	2.1	76.2	11.0	1.4	6.5	3.0	1.8

[a] All of the copolymer samples except for this T3(AA) were prepared at M_P/M_E = 1. This T3(AA) sample was prepared at M_P/M_E = 4/6. [b] Randall method. [c] Kakugo method.

Table VI

Triad Sequence Distribution of Ethylene–Propylene Copolymers and Reactivity Ratios of Monomers Predicted by Using the First-Order Markov Model

catalyst	method	EEE	PEE	PEP	EPE	PPE	PPP	r_E	r_P	r_Er_P	SS[d] × 10^4
T3ME	R[b]	76.2	13.9	0.6	6.2	2.7	0.3	10.95	0.22	2.42	8.74
	K[c]	74.3	15.0	0.8	6.8	2.9	0.3	9.94	0.21	2.09	7.39
T3MD2	R	71.0	16.8	1.0	7.9	3.0	0.3	8.46	0.19	1.60	7.01
	K	69.4	17.7	1.1	8.5	3.0	0.3	7.85	0.18	1.39	12.94
T3MED4	R	73.5	15.7	0.8	7.7	2.1	0.1	9.34	0.14	1.29	2.01
	K	72.6	16.2	0.9	8.0	2.1	0.1	8.95	0.13	1.20	9.63
T3MED8	R	73.8	15.5	0.8	7.4	2.3	0.2	9.54	0.16	1.50	2.38
	K	73.2	15.8	0.9	7.6	2.3	0.2	9.26	0.15	1.41	6.19
T3MED12	R	67.8	18.3	1.2	8.5	3.7	0.4	7.41	0.22	1.61	4.28
	K	68.5	17.9	1.2	8.3	3.7	0.4	7.63	0.23	1.72	21.19
T3(AA)	R	64.9	18.5	1.3	7.4	6.4	1.4	7.00	0.44	3.05	17.09
	k	63.7	19.2	1.4	7.8	6.5	1.4	6.64	0.42	2.80	24.77
T3(AA)[a]	R	77.2	13.1	0.6	5.5	3.3	0.5	11.80	0.30	3.51	9.58
	K	76.7	13.3	0.6	5.6	3.3	0.5	11.53	0.30	3.43	9.05

[a] All copolymer samples except for this T3(AA) were prepared at M_P/M_E = 1. This T3(AA) sample was prepared at M_P/M_E = 4/6. [b] Triad sequence distribution predicted from the observed dyad sequence distribution by the Randall method. [c] Triad sequence distribution predicted from the observed dyad sequence distribution by the Kakugo method. [d] Sum of squares of deviation from the observed value (mole fraction) in Table V.

favored by the propylene activity for homopolymerization.

Molecular Weight Distribution (MWD). Figure 7 shows the molecular weight distribution measured by gel permeation chromatography for copolymers at M_P/M_E = 1. The T3ME catalyst gives the narrowest distribution, whose polydispersity ($\bar{M}_w/\bar{M}_n$) is 2.57. Other catalysts show rather broader distribution ($\bar{M}_w/\bar{M}_n \cong 5$). If the catalyst has only a single active species, the polydispersity of polymer obtained is known to be 2. It is believed that the MWD of copolymers becomes broader probably due to the formation of active species of more than one type in the catalyst by removal of THF from T3ME.

Microstructure of Ethylene–Propylene Copolymer. The microstructure of copolymer is one of the most important factors determining the physical properties of copolymer. ^{13}C NMR is one of the most powerful analytical methods to evaluate the microstructure of ethylene–propylene copolymers.

Figure 8 shows typical ^{13}C NMR spectra of copolymers. The assignments[17,27] for each chemical shift are listed in Table IV. Figure 8 and Table IV show that the peak due to the sequence of propylene (PPPP) in S$\alpha\alpha$ (46–47 ppm) and the peaks due to the sequence of propylene (PPP) in T$\beta\beta$ (28.7 ppm) and P$\beta\beta$ (21–22 ppm) are not found from the copolymer obtained with T3ME (Figure 8A) and T3MED*X* (*X* = 2, 4, 8) catalysts, but these peaks do appear in the copolymer obtained with T3MED12 (Figure 8B) and $TiCl_3$(AA) catalysts. These differences are also shown in Tables V and VI.

Table V shows dyad–triad sequence distribution of copolymer observed from the data of Table IV by following the methods proposed by Randall[17] and Kakugo.[18] Both methods show good agreement. The reactivity ratios of monomers in Table VI are estimated from the observed dyad sequence distribution of Table V on the assumption that the copolymerization is a first-order Markovian process. The triad sequence distributions of copolymer in Table VI are predicted from the first-order Markovian model. The sums of the squares of the deviation from observed value in Table VI are less than 10 × 10^{-4} except that for $TiCl_3$(AA), which indicates the applicability of the Markovian model.[28]

As shown in Table VI, the product of reactivity ratio (r_Er_P) of the T3MED4 catalyst is lower than that of T3ME, while those of T3MED12 and $TiCl_3$(AA) are higher than that of T3MED4. Table VI and Figure 4 also show that the effects of THF removal on the product of reactivity ratios and stereospecificity of polypropylene are in the same trend.

From the results of ^{13}C NMR study on the removal of THF from T3ME catalyst, it seems that the multinuclear Ti^{3+} species as in T3MED12 and $TiCl_3$(AA) favors the formation of propylene blocks in copolymer while the isolated Ti^{3+} species favors the random insertion of propylene into the ethylene main chain. The random insertion of propylene by isolated Ti^{3+} species is more favored for T3MED4 with vacancies than for T3ME with vacant sites occupied by THF.

Conclusion. $TiCl_3(AA)/MgCl_2$/THF (T3ME) catalyst was prepared, and THF was removed by DEAC to make four different catalysts with different THF contents (T3MED2, T3MED4, T3MED8, T3MED12). The effect of THF removal was analyzed in terms of the state of the Ti^{3+} species. XRD and ESR studies suggested that with THF removed the isolated Ti^{3+} species as in T3ME changes into multinuclear Ti^{3+} species as in T3MED12.

Multinuclear Ti^{3+} species (T3MED12, $TiCl_3$(AA)) contribute to the increase of I.I. and activity in the propylene polymerization, the relative activity of propylene, and the formation of propylene blocks in ethylene–propylene copolymerization. On the other hand, isolated Ti^{3+} species (T3ME, T3MED2, T3MED4) contribute to the increase of activity in the ethylene polymerization and the random insertion of propylene into the ethylene main chain in ethylene–propylene copolymerization.

For isolated Ti^{3+} species, the vacancies of T3ME are filled with THF while those of T3MED4 are empty due to THF removal. In comparison with T3ME catalyst, T3MED4 catalyst shows higher activity in ethylene homopolymerization, higher randomness of propylene unit in copolymer, and lower isotactic index of polypropylene.

It was found that with THF removed the MWD of ethylene–propylene copolymers became broader, probably due to the formation of active species of more than one type in the catalysts.

References and Notes

(1) Karol, F. J. *Catal. Rev. Sci. Eng.* **1984**, *26*, 557–595.
(2) Chien, J. C. W. *Catal. Rev. Sci. Eng.* **1984**, *26*, 613–629.
(3) Hsieh, H. L. *Catal. Rev. Sci. Eng.* **1984**, *26*, 631–651.
(4) Choi, K. Y. *J. Macromol. Sci., Rev. Macromol. Chem. Phys.* **1985**, *C25*, 1–55.
(5) Barbe, P. C.; Cecchin, G.; Noristi, L. *Adv. Polymn. Sci.* **1987**, *81*, 1–79.
(6) Wu, Q.; Yang, N. L.; Lin, S. *Makromol. Chem.* **1990**, *191*, 89–97.
(7) Soga, K.; Uozumi, T.; Park, J. R. *Makromol. Chem.* **1990**, *191*, 2853–2864.
(8) Karol, F. J.; Cann, K. J.; Wagner, B. E. Developments with High Activity Titanium, Vanadium, and Chromium Catalysts in Ethylene Polymerization. *Proceedings*, Internation Symposium, Hamburg; Springer-Verlag: Berlin, Heidelberg, 1987; pp 149–161.
(9) Wertz, J. E.; Bolton, J. R. *Electron Spin Resonance, Elementary Theory and Practical Applications*; McGraw-Hill: New York, 1972; pp 17–36.
(10) Keszler, B.; Bodor, G.; Simon, A. *Polymer* **1980**, *21*, 1037–1040.
(11) Dumas, C.; Hsu, C. C. *J. Macromol. Sci., Rev. Macromol. Chem. Phys.* **1984**, *C24*, 355–386.
(12) Cozewith, C.; Strate, G. V. *Macromolecules* **1971**, *4*, 482–489.
(13) Soga, K.; Yanagihara, H.; Lee, D. H. *Makromol. Chem.* **1989**, *190*, 37–44.
(14) Peng, D. Y.; Robinson, D. B. *Ind. Eng. Chem. Fundam.* **1976**, *15*, 59.
(15) Burfield, D. R.; Loi, P. S. T. *Stud. Surf. Sci. Catal.* **1985**, *25*, 387–406.
(16) Tosi, C.; Simonazzi, T. *Angew. Macromol. Chem.* **1973**, *32*, 153–161.
(17) Randall, J. C. *J. Macromol. Sci., Rev. Macromol. Chem. Phys.* **1989**, *C29*, 201–317.
(18) Kakugo, M.; Naito, Y.; Mizunuma, K.; Miyatake, T. *Macromolecules* **1982**, *15*, 1150–1152.
(19) Zakharov, V. A.; Makhtarulin, S. I.; Polubojarov, V. A.; Anufrienko, V. F. *Makromol. Chem.* **1984**, *185*, 1781–1793.
(20) Chien, J. C. W.; Wu, J. C. *J. Polym. Sci., Polym. Chem. Ed.* **1982**, *20*, 2461–2476.
(21) Wertz, J. E.; Orton, J. W.; Auzins, P. *Discuss. Faraday Soc.* **1961**, *31*, 140–155.
(22) Tsutsui, T.; Kashiwa, N. *Polym. Commun.* **1988**, *29*, 180–183.
(23) Tait, P. J. T.; Downs, G. W.; Akinbami, A. A. Presented at the Meeting of the American Chemical Society, Akron, OH, 1986.
(24) Mayo, F. R.; Lewis, F. M. *J. Am. Chem. Soc.* **1944**, *66*, 1594–1601.
(25) Randall, J. C. *Polymer Sequence Determination Carbon-13 NMR Method*; Academic Press: New York, 1977; pp 71–78.
(26) Nowlin, T. E.; Kissin, Y. V.; Wagner, K. P. *J. Polym. Sci. Part A: Polym. Chem.* **1988**, *26*, 755–764.
(27) Cheng, H. N. *Macromolecules* **1984**, *17*, 1950–1955.
(28) Cozewith, C. *Macromolecules* **1987**, *20*, 1237–12441.

Registry No. THF, 109-99-9; PE, 9002-88-4; $TiCl_3$, 7705-07-9; $MgCl_2$, 7786-30-3; (ethylene)(propylene) (copolymer), 9010-79-1; polypropylene, 9003-07-0; ethylene, 74-85-1; propylene, 115-07-1.